Quantitative Strength Prediction of Advanced Ceramics With Regular/Irregular Flaws in I-Mode Condition

Xinyuan Zhao
Nanjing Institute of Technology
Anzhe Wang (wanganzhe14b@126.com)
Nanjing Institute of Technology
Yaoyu Chen
Nanjing Institute of Technology
Qihan Zheng
Nanjing Institute of Technology

Research Article

Keywords: Ceramic, Irregular flaw, Strength prediction, Finite element simulation, Laser processing

Posted Date: May 20th, 2021

DOI: https://doi.org/10.21203/rs.3.rs-537231/v1

Quantitative strength prediction of advanced ceramics with regular/irregular flaws in I-mode condition

Xinyuan Zhao[a], Anzhe Wang[1]*[a,b], Yaoyu Chen[a], Qihan Zheng[a]

[a] School of Materials Science and Engineering, Nanjing Institute of Technology, Nanjing 211167, P. R. China

[b] Jiangsu Key Laboratory of Advanced Structural Materials and Application Technology, Nanjing 211167, P. R. China

Abstract: Flaws in ceramics have a significant impact on their strength. Realization of ceramic strength from qualitative statistical description to quantitative prediction is essential for the fields of fracture mechanics, materials science and engineering applications. In this study, two regular flaw-strength prediction models with clear physical meaning were established under I-mode failure according to the classic crack-strength model (Sato [17]) combined with two critical stress intensity factor K_c vs. tip radius r relationships (Gómez [18] and Yang [19]). Comparison with the data that reported in the literature proved that the Sato-Yang model was more accurate than the Sato-Gómez model. On the basis of finite element simulation and mathematical fitting, a simple coefficient that can reasonably described the complexity of flaw shapes was proposed, thus extending the regular flaw-strength model to solve the irregular flaw problem and passing the experimental verification at the same time.

Keywords: Ceramic; Irregular flaw; Strength prediction; Finite element simulation; Laser processing

***Corresponding author*: Tel/fax: +86 025 86118275**
E-mail address: wanganzhe14b@126.com (A.Z. Wang)

1. Introduction

The prediction of ceramic fracture has always been a hot research topic both in the fields of fracture mechanics and engineering technology owing to the intrinsic brittleness, high inherent strength and low fracture toughness of ceramics [1-5]. All ceramics have an inherent population of flaws (also called defects) caused by processing, sintering, presintered or solid state sintered ceramic machining and handling, thus leading to a scatter of the strength depending on the flaw types (e.g. cracks, pores, scratches, edge chipping, inclusions and coarse grains), sizes (submicron to millimeter level) and shapes (sharp to blunt) [6]. Currently, more attention is focused on the problem of surface flaws due to the fact, discovered by statistical studies [7], that as the size of the defect increases and the location approaches the surface, a more serious strength attenuation will occur in ceramics.

Numerous models have been proposed to describe the effect of surface flaw size and shape on fracture strength σ_f, which mainly focused on the semi-circular or semi-elliptical crack problems [8-11]. However, a large part of defects in actual ceramics are pores and machining flaws, while the crack problem is often only an extreme case, because it is the sharpest (tip radius reaches the atomic level), thus resulting in the highest degree of stress concentration. According to the literature [12,13], the cross-sectional morphology of flaws in ceramics is irregular in most cases, while semi-circular and semi-elliptical defects (as shown in Fig. 1a and b), which can be described by existing theories and models, are relatively rare. Not only the complexity of the cross-sectional shape, these defects are much more complicated than cracks because of the variety of the tip radius. At present, both theoretical and experimental studies mainly focus on the typical crack problems, while there are few reports on the flaw cases which are more common and complex. Considering the particularity of the crack problem, the current research achievements cannot be directly applied in a more general sense.

In view of this, we have recently done some explorations, which is based on the classic crack model, and established the cross-sectional area-related pore-like flaw-strength response model by considering the critical stress intensity factor vs. tip

radius (K_c-r) relationship [14]. Subsequently, the model's applicability is investigated through the control variable method (independently changing the defect length or depth to change the area value), and it is found that although the proposed model has good accuracy, there exist some deviations that cannot be ignored in the prediction accuracy of different fine ceramics. Furthermore, the strength prediction accuracy under the action of small-sized pores is insufficient.

Therefore, (*i*) developing a new quantitative flaw-strength prediction model with higher accuracy and wider applicability for ceramics is of great practical significance for further promoting the reliable application of fine ceramics and broadening its application range. (*ii*) In addition, in light of the shape anisotropy of inherent flaws in ceramics, it is necessary to consider the applicability of the proposed model to all flaws. In other words, can all flaws only take into account their cross-sectional area value to predict the fracture strength? From the premise of the model derivation, it can be found that the classic crack-strength model is derived based on the crack with symmetric and regular cross-sectional shape [15]. When the cross-sectional shape becomes asymmetric and irregular, which is the most common case of inherent flaws, the hypothetical precondition will not hold.

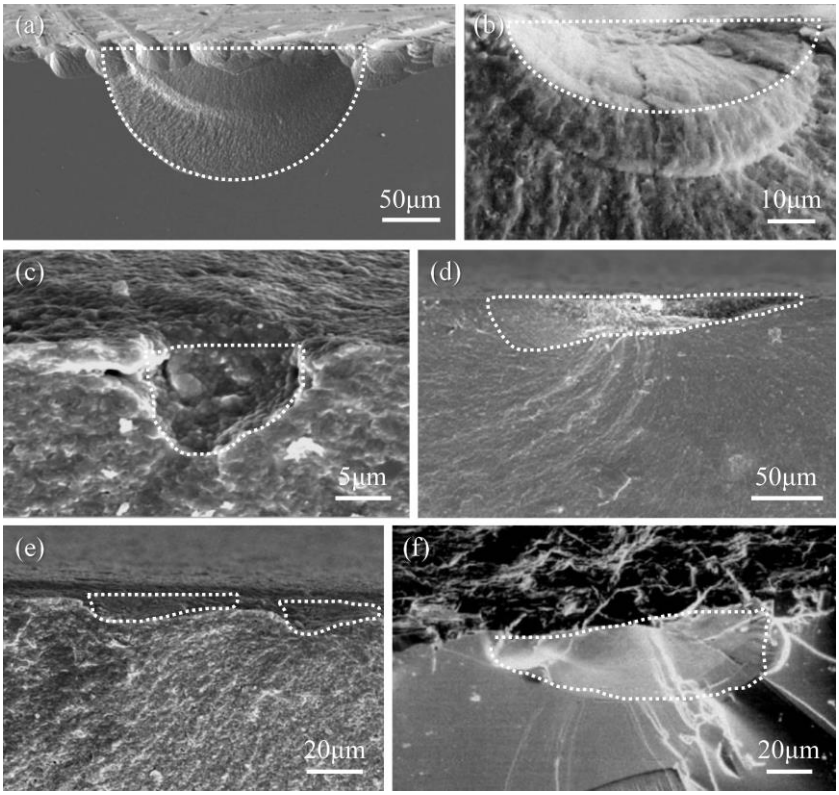

Fig. 1. Examples of actual flaws at fracture origins of dense ceramics. (a) edge chipping in 3Y-TZP ceramic [6], (b) critical grinding flaw in fine grain $MgAl_2O_4$ [13], (c) surface pore in 3Y-TZP, (d,e) critical grinding flaw in 3Y-TZP [12] and (f) machining chipping in large grain transparent Y_2O_3 ceramic [13].

The aim of this study is to develop a more universal model for the quantitative strength prediction in ceramics. For regular flaw problem, the accuracy and applicability of the new and old models were firstly discussed based on our previous research data. Then, the regular flaw-strength model with higher accuracy is extended to the irregular defect problem on the basis of finite element simulation and mathematical fitting, and verified by experiments.

2. Experimental

Precisely polished 5 mol% yttria-stabilized tetragonal zirconia polycrystal (5Y-TZP), Si_3N_4 and SiC ceramic samples with the size of 3 × 4 × 45 mm^3 were provided by Zhu-hai Jiawei Ceramic Technology Co., Ltd. ZrB_2-SiC ceramic bars were self-made and the preparation procedures were described elsewhere [16]. Surface flaws with regular shapes were fabricated by laser processing approach (Fig. 2a and b) and the detailed procedures can be found in Ref. [14]. Defects with different depths at both ends (so-called irregular flaws) were introduced by placing a thin metal gasket under one side of the sample during laser processing (see Fig. 2c).

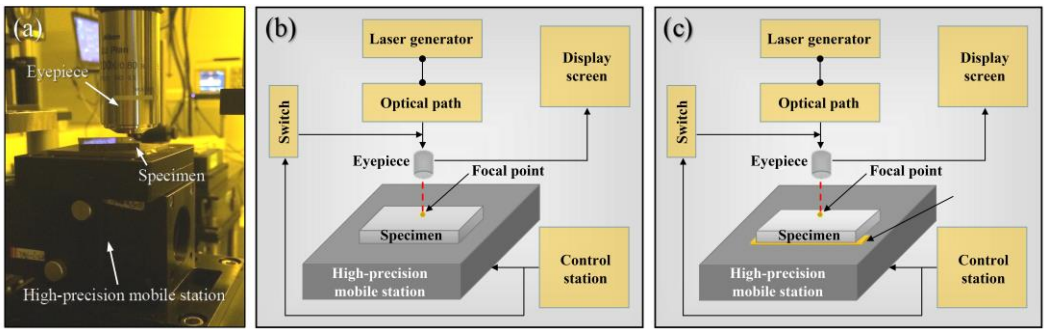

Fig. 2. Laser processing method: (a) physical photo and the Schematic diagrams of the introduction of (b) regular as well as (c) irregular flaws.

3. Regular flaw-strength response

Before modeling the irregular flaw-strength relationship, it is generally necessary to obtain an accurate solution of the regular flaw problem, and then solve the irregular

flaw problem by considering the shape coefficient. Thus, our work start with the regular flaw-strength modeling. It should also be noted that the following work is carried out under the I-mode condition.

3.1. Modeling on the regular flaw problem

Fracture strength of ceramics containing a regular cross-sectional crack in mode I condition is expressed as follows (proposed by Sato *et al.*) [17]:

$$\sigma_{fr-crack} = \frac{2\sigma_0}{\pi}\cos^{-1}\left(\frac{8n^2\sigma_0^2\sqrt{area}}{\pi \cdot K_{Ic}^2 + 8n^2\sigma_0^2\sqrt{area}}\right) \tag{1}$$

where σ_0 is the original strength, K_{Ic} is the fracture toughness, *area* is the area of a surface crack projected onto the direction of the maximum tensile stress, n is a dimensionless coefficient related to Poisson's ratio (v). The reason why this model is only suitable to regular cracks is that it is derived on the basis of the Murakami-Endo model [15], which is merely applicable to the regular and symmetrical cracks as shown in Fig. 3 (such as rectangular, semi-circular and semi-elliptical *et al.*).

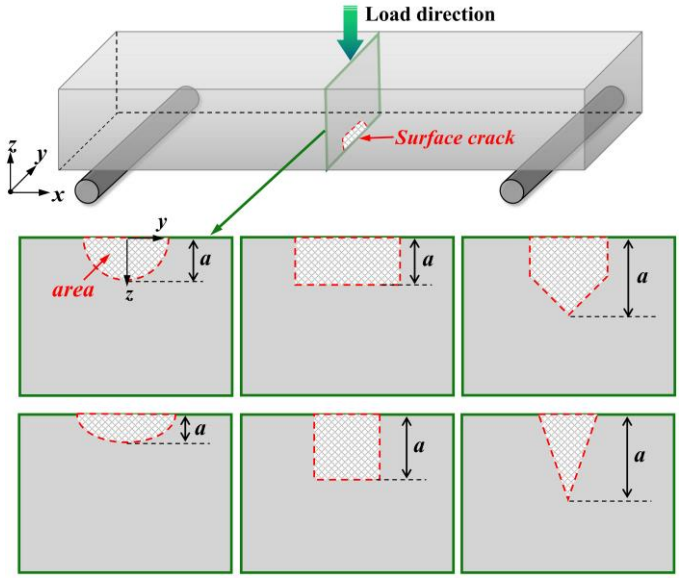

Fig. 3. Fracture surfaces of typical cracks with regular and symmetrical shapes.

Supposing that both crack and other typical flaws are damaged and cause fracture when maximum stress reaches the critical value (material constant), the crack problem can be transformed into a common flaw problem by introducing K_c-r coefficient. Here, drawing on the K_c-r relationships proposed by Gómez [18] and Yang [19], the following two regular flaw-strength models are obtained respectively:

Sato-Gómez model: $$\sigma_{fr-flaw}=\frac{2\sigma_0}{\pi}\cos^{-1}\left(\frac{8n^2\sigma_0^2\sqrt{area}}{\pi\cdot K_{Ic}^2+8n^2\sigma_0^2\sqrt{area}}\right)\times\sqrt{1+\frac{\pi r}{4}\left(\frac{\sigma_0}{K_{Ic}}\right)^2} \quad (2)$$

Sato-Yang model: $$\sigma_{fr-flaw}=\frac{2\sigma_0}{\pi}\cos^{-1}\left(\frac{8n^2\sigma_0^2\sqrt{area}}{\pi\cdot K_{Ic}^2+8n^2\sigma_0^2\sqrt{area}}\right)\times\beta\sqrt{1+\frac{r}{1.12^2\times 4\pi G}} \quad (3)$$

where r is the tip radius of flaw in the direction perpendicular to the maximum tensile stress, G is the average grain size, and β is the material constant. The Eq. (2) has been proved to have some deviations that cannot be ignored in strength prediction of different fine ceramics in Ref. [14]. Therefore, we have higher expectations for the Eq. (3), because the β value is a variable (ranging from 0.7 to 1.3) reflecting the material properties.

3.2. Comparison and analysis

The Sato-Yang model (Eq. (3)) strongly relies on obtaining the β value. Here, linear fitting are conducted on our previous test results (reported in Ref. [20]), and the β values of ZrB_2-SiC, ZrB_2, 5Y-TZP and SiC are obtained as 1.08, 0.962, 0.719 and 0.903 (see Fig. 4), respectively, which are consistent with the range from 0.7 to 1.3 reported by Yang *et al* [19].

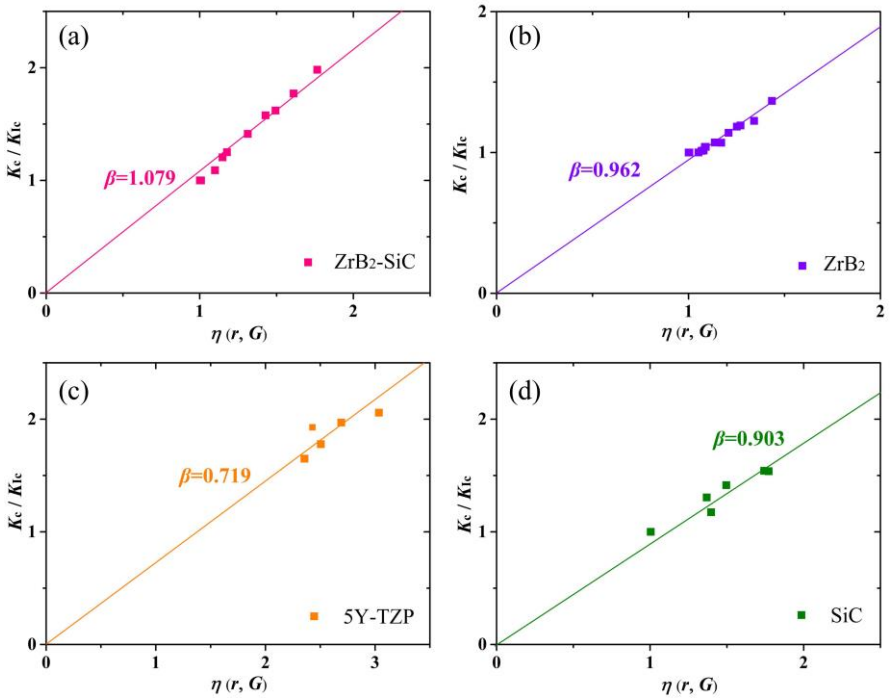

Fig. 4. The β values of (a) ZrB_2-SiC, (b) ZrB_2, (c) 5Y-TZP and (d) SiC ceramics obtained by linear regression.

Fig. 5a-c shows the comparison between the prediction results of the two models and the measured values in Ref. [14]. It can be found that both of them have almost the same overall trend except for slight deviations in strength prediction values. After comparing with the as-reported experimental results, it is noteworthy that the comprehensive accuracy of the Sato-Yang model is relatively higher. For example, for Si_3N_4 flaws with a cross-sectional area of about 1000 μm^2, the tested average strength is 651 MPa, and the predicted values of Sato-Yang and Sato-Gómez are 570 MPa and 607 MPa, respectively. The accuracy of the latter reaches 93.2% (increased by 5.7% compared to the former). Fracture morphology in Fig. 5d indicates that the *area* of defects are all symmetrical and regular.

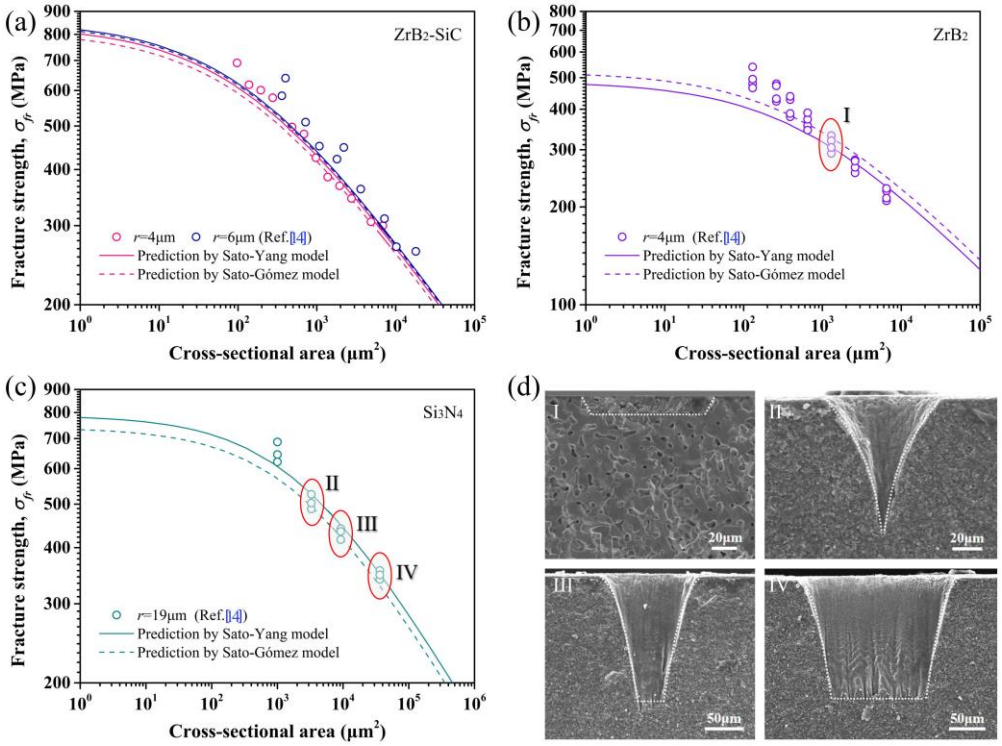

Fig. 5. (a-c) Comparisons between the prediction results of the Sato-Yang and Sato-Gómez models as well as the experimental values, and (d) the fracture morphologies of typical test samples.

4. Irregular flaw-strength response

The purpose of this section is to explore the applicability of the regular flaw-strength model in irregular defect problems. Since the introduction of irregular flaws is more difficult than that of regular defects, the research is mainly conducted by simulation method. It is worth noting that the contour lines of irregular defects in

Fig. 1c-f are generally trapezoid-like. In order to facilitate the parameterization of the model, we simplify the cross-sectional shape of this kind of irregular defects to trapezoid.

4.1. Finite element simulation (FEM)

The criteria for judging material failure include critical stress (σ_c) method and critical stress intensity factor (K_c) method, etc. However, the latter may not suitable in small flaw cases because the K_c is not constant and tends to become smaller for smaller flaws [21-23]. So the critical stress criterion is utilized for the subsequent simulation.

The model is created using a commercial FEM code ANSYS 18.2 for ZrB_2-SiC ceramic. The simulation assume an elastic modulus of 400 GPa and a Poisson's ratio of 0.12 [24,25]. Four-node plane elements are used in the analysis and the minimum mesh size is about 3 μm, see Fig. 6a. The total number of nodes and elements in the finite element analysis are 1.35×10^6 and 9.8×10^5, respectively. The σ_c is taken as 740 MPa [14,26], and the stress distribution around the flaw under critical failure conditions is shown in Fig. 6b. Results in Table 1 indicate that the fracture strength obtained by FEM method compared well with the experimental results (average error is only 3.8%).

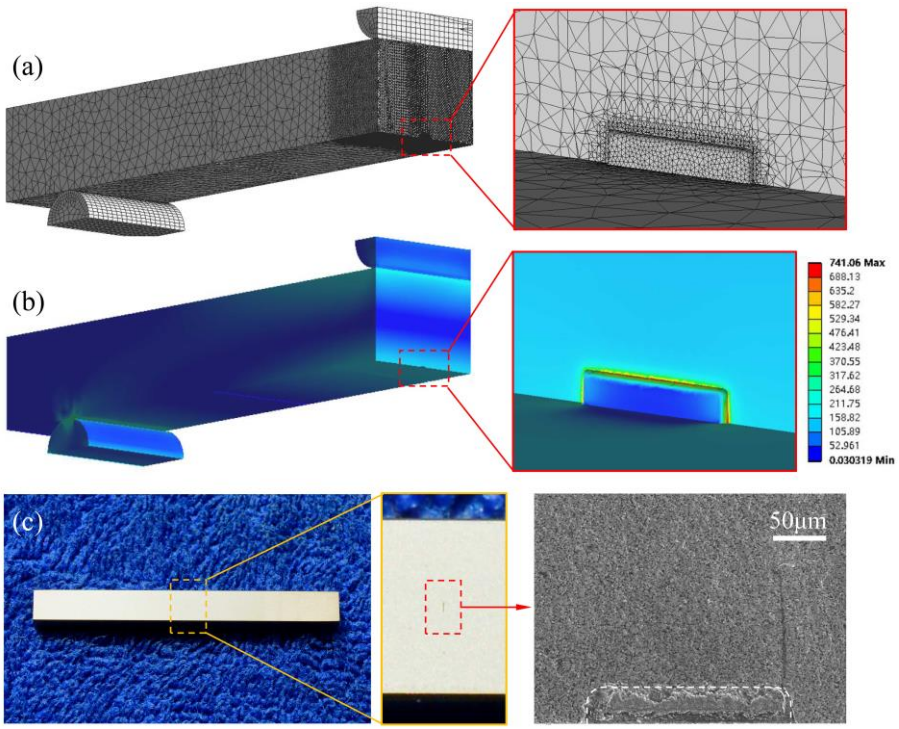

Fig. 6. A typical flaw with the length of 200 μm and the depth of 36 μm. (a) Grid distribution in FEM, (b) stress distribution after simulation and (c) the images of the laser-introduced flaw before and after fracture.

Table 1 Fracture strength of ZrB_2-SiC sample containing regular flaws obtained by simulations and experiments

Abbreviation	Flaw length, $2c$ (μm)	Flaw depth, a (μm)	Tip radius, r (μm)	Fracture strength, σ_{fr} (MPa)		Error (%)
				Experimental results [14]	FEM results in this work	
ZS-I	500	36	6	260	245.6	5.5
ZS-II	200	36	6	279	273.1	2.1
ZS-III	200	12	4	365	351.3	3.8

Based on the above comparison, it is reasonable to believe the reliability of the simulation results. On this basis, the flaw-strength response simulations under the same cross-sectional area value while different cross-sectional shapes are carried out subsequently. It is clear that the unsymmetric flaws lead to the unsymmetric stress-intensity distributions, and the fracture strength decay rapidly with the increase of flaw angle θ, then change smoothly when θ exceeded 5° (see Fig. 7).

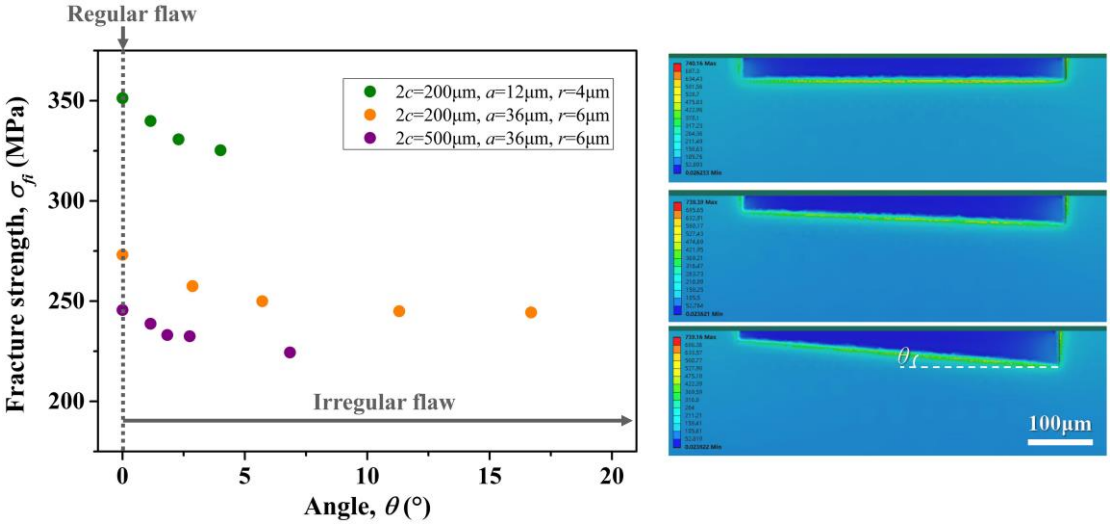

Fig. 7. Relationship between the fracture strength caused by irregular flaws (σ_{fi}) and the flaw angle θ, and the typical stress distribution cloud diagram.

4.2. Modeling on the irregular flaw problem

Generally, the shape of a trapezoid can be described by the slope of its hypotenuse (that is, the bottom edge of the flaw) or the corresponding trigonometric function. Here, taking $sin\theta$ as the abscissa, it is interesting that, in Fig. 8a, the σ_{fi}/σ_{fr}

values follow almost the same attenuation law and seem irrelevant with the sizes as well as shapes of the flaws. In order to facilitate modeling, the fitting result is expected to pass through the origin. Theoretically, the irregular flaw problem could turn into the regular one when θ is 0°. In this case, σ_{fi} is equal to σ_{fr}, and the strength ratio (σ_{fi}/σ_{fr}) is 1. Thus, 1-σ_{fi}/σ_{fr} can be regarded as the dependent variable (i.e. ordinate), and the Fig. 8a can be transformed into Fig. 8b. Here, power-law fitting is used to obtain the best fit for the data, and the exponent of the power-law is about 0.4. Therefore, the fracture strength in irregular flaw cases, σ_{fi}, can be expressed as:

$$\sigma_{fi} = [1 - 0.185(\sin\theta)^{0.4}] \cdot \sigma_{fr} \tag{4}$$

where σ_{fr} is the strength prediction value based on the regular flaw-strength model (Eqs. (2) or (3)) under the same cross-sectional area condition.

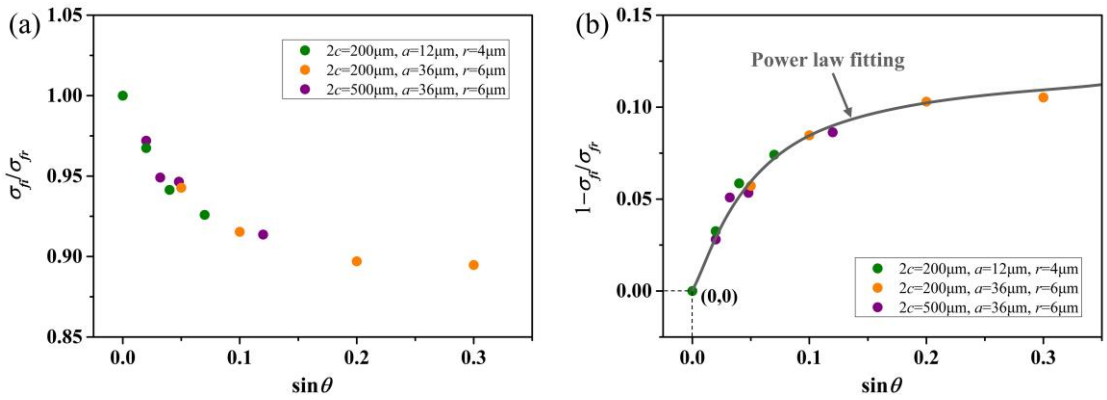

Fig. 8. (a) The σ_{fi}/σ_{fr} vs. $sin\theta$ relationship and (b) the power-law relationship between 1-σ_{fi}/σ_{f} and $sin\theta$.

4.3. Experimental verification

Two trapezoid-like flaws are successfully introduced into 5Y-TZP and SiC ceramics via laser approach, and the strength values obtained by three-point bending are 332 MPa and 171 MPa, respectively. According to the fracture morphology in Fig. 9, the defect cross-sectional areas in 5Y-TZP and SiC ceramics are about 86757 μm^2 and 18032 μm^2, and the $sin\theta$ are ~0.471 and ~0.286, respectively. The predicted strengths are 293 MPa (error of 12%) and 185 MPa (error of 8%) using Eqs. (2) and (4), while the results predict from Eqs. (3) and (4) are 354 MPa (error of 7%) and 170 MPa (error of 1%). The above results indicate that the Eq. (4), which is simple in form, has high accuracy, especially when based on the Sato-Yang model.

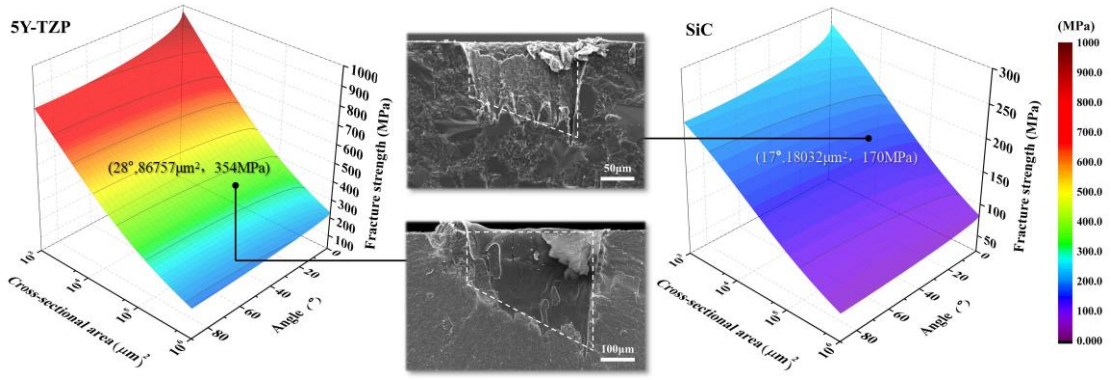

Fig. 9. Comparison between the prediction results of the Eq. (4) based on the Sato-Yang model and the experimental values of 5Y-TZP and SiC ceramics.

5. Discussion

After comparing the experimental results with the predicted values of the Sato-Gómez and Sato-Yang models, it is clear that the latter one is relatively more precise. The possible reasons are: (*i*) The Sato-Gómez model attempts to cover all ceramic materials, resulting in a large error in the K_c-r relationship near the critical tip radius. It can be seen from Fig. 1b in the Ref. [18] that the approximation degree of the model to the measured data of various ceramics is significantly different near the critical tip radius. (*ii*) Furthermore, the K_c-r relationship coefficient is more dependent on the intrinsic strength and fracture toughness measurement values when using Sato-Gómez model. At this moment, the deviation of the intrinsic strength measurement value will be amplified, thus leading to a larger strength prediction error.

Comparing the Sato-Gómez and Sato-Yang models, it should be pointed out that there exist a critical tip radius r_c by combining Eqs. (2) and (3) :

$$r_c = \frac{4\pi G \cdot (\beta^2 - 1) \cdot (1.12K_{Ic})^2}{(1.12\pi\sigma_0)^2 \cdot G - (\beta K_{Ic})^2} \tag{5}$$

As r deviates from r_c, the prediction error of the Sato-Gómez model increases gradually. It cannot be ignored that the prediction accuracy of the Sato-Yang model is sometimes lower than that of the Sato-Gómez model, such as the small-sized flaw cases in ZrB_2 ceramic. Taking the porous properties of ZrB_2 into account, the fracture strength response will be greatly affected by the inherent micropores when the

cross-sectional area of the artificial flaw is too small (less than 500 μm^2 in Fig. 5b), and thus the fracture strength tends to be the intrinsic strength. When the cross-sectional area increases, the prediction accuracy of the Sato-Yang model improves significantly. For dense ceramics, such as ZrB_2-SiC and Si_3N_4 in Fig. 5a and c, the Sato-Yang model also indicates good prediction accuracy regardless of whether the flaw is large or small (cross-sectional area ranging from 10^2 to 10^5 μm^2). In actual situations, results sometimes show that the Sato-Gómez model fits better than the Sato-Yang model due to the dispersion of strength, but based on more test data, it is reasonable to believe that the the latter one is generally more accurate in strength prediction. However, the shortcoming of the Sato-Yang model is that the acquisition of β values (between 0.7 and 1.3 [19]) is troublesome, which requires researchers to provide more comprehensive material data.

It should be noted that our present work only focuses on type I fractures. Nevertheless, the orientation and location of inherent flaws in ceramics are randomness, and the actual failure situation could be more complicated. Although many strength prediction models under mixed fracture modes have proposed in the past decades, such as the maximum stress criterion and the maximum strain energy criterion, and our previous studies [26] have confirmed that the latter has obvious advantages in predicting regular defects-strength, such research on irregular flaw problem has not yet to be carried out. Considering that the maximum stress position is no longer clear because irregular flaws always leading to unsymmetric stress-intensity distributions, the strength prediction will be more complicated when facing the problem of irregular flaws combined with mixed fracture mode. Nevertheless, a major breakthrough in this work is to construct a relationship which describing the response of strength with irregular flaws by simplifying the very common surface pores and processing defects to trapezoidal-like cross-sectional flaws, and thus realizing the quantitative strength prediction in mode I condition by a simple equation.

6. Conclusions

In this study, the physical nature of flaw-induced cracking, which leads to the random distribution of the strength in advanced ceramics, is investigated based on

modeling, simulation and experiment, and the conclusions are as follows: The regular flaw-strength prediction model is not applicable to the problem of irregular defects, while the latter case is more harmful to strength. The Sato-Yang model shows good prediction precision for a variety of dense ceramics, and thus a closed-loop could be effectively formed including flaw detection (such as non-destructive testing), hazard determination (this work), material screening and selection, and reliable application (ultimate purpose). This work brings about a new strength prediction model for the field of fracture mechanics and provides a potential material screening criterion for the engineering application of ceramics at the same time.

Acknowledgement

Financial support was provided by the Natural Science Foundation of Jiangsu Province (No. BK20201040), the Special Talent Introduction for "Double Innovation Plan" in 2019, the National Natural Science Foundation of China (No. 51801098), the Open Research Fund of Anhui Key Laboratory of High-Performance Non-ferrous Metal Materials, the University Research Foundation of Nanjing Institute of Technology (No. YKJ201806) and the Outstanding Scientific and Technological Innovation Team in Colleges and Universities of Jiangsu Province.

References

[1] S. Ozaki, Y. Aoki, T. Osada, *et al*., Finite element analysis of fracture statistics of ceramics: effects of grain size and pore size distributions, J. Am. Ceram. Soc. 101 (2018) 3191-3204.

[2] J. Lamon, 1-Flaws in materials, Brittle fracture and damage of structural ceramics & composites, 2016, 1-33.

[3] A.G. Evans, Fracture mechanics determinations, concepts, flaws, and fractography, Springer, US, 1974.

[4] H.M. Xiang, Y. Xing, F.Z. Dai, *et al*., High-entropy ceramics: Present status, challenges, and a look forward, J. Adv. Ceram. 10 (2021) 385-441.

[5] J.X. Liu, X.Q. Shen, Y. Wu, *et al*., Mechanical properties of hot-pressed high-entropy diboride-based ceramics, J. Adv. Ceram. 9 (2020) 503-510.

[6] I. Denry, How and when does fabrication damage adversely affect the clinical

performance of ceramic restorations? Dent. Mater. 29 (2013) 85-96.

[7] S.S. Scherrer, U. Lohbauer, A. Della Bona, *et al*., ADM guidance—Ceramics: guidance to the use of fractography in failure analysis of brittle materials, Dent. Mater. 33 (2017) 599-620.

[8] T. Fett, Stress intensity factors for semi-elliptical surface cracks in a plate under tension based on the Isida's solution, Int. J. Fract. 48 (1991) 139-151.

[9] I.S. Raju, J.C. Newman Jr., Stress-intensity factors for a wide range of semi-elliptical surface cracks in finite-thickness plates, Eng. Fract. Mech. 11 (1979) 817-829.

[10] S. Strobl, P. Supancic, T. Lube, *et al*., Surface crack in tension or in bending-a reassessment of the newman and raju formula in respect to fracture toughness measurements in brittle materials, J. Eur. Ceram. Soc. 32 (2012) 1491-1501.

[11] S. Kolitsch, H.P. Gänser, R. Pippan, Approximate stress intensity factor solutions for semi-elliptical cracks with large a/W and c/B under tension and bending, Theor. Appl. Fract. Mech. 92 (2017) 167-177.

[12] S.S. Scherrer, M. Cattani-Lorente, E. Vittecoq, *et al*., Fatigue behavior in water of Y-TZP zirconia ceramics after abrasion with 30 μm silica-coated alumina particles, Dent. Mater. 27 (2011) e28-e42.

[13] R.W. Rice, Monolithic and composite ceramic machining flaw-microstructure-strength effects: model evaluation, J. Eur. Ceram. Soc. 22 (2002) 1411-1424.

[14] A.Z. Wang, P. Hu, X.Y. Zhao, Xinyuan, *et al*., Modelling and experimental investigation of pore-like flaw-strength response in structural ceramics, Ceram. Int. 10 (2020) 14431-14438.

[15] Y. Murakami, M. Endo, Quantitative evaluation of fatigue strength of metals containing various small defects or cracks, Eng. Fract. Mech. 17 (1983) 1-15.

[16] A.Z. Wang, P. Hu, X.H. Zhang, *et al*., Accurate measurement of fracture toughness in structural ceramics, J. Eur. Ceram. Soc. 37 (2017) 4207-4212.

[17] N. Sato, K. Takahashi, Evaluation of fracture strength of ceramics containing small surface defects introduced by focused ion beam, Materials 11 (2018) 457.

[18] F.J. Gómez, G.V. Guinea, M. Elices, Failure criteria for linear elastic materials with U-notches, Int. J. Fract. 141 (2006) 99-113.

[19] S.G. Yang, C.G. Zhang, X.C. Zhang, Notch radius effect on fracture toughness of ceramics pertinent to grain size, J. Eur. Ceram. Soc. 40 (2020) 4217-4223.

[20] A.Z. Wang, X.Y. Zhao, M.X. Huang, *et al*., A systematic study on the quality improving of fracture toughness measurement in structural ceramics by laser notching method, Theoretical and Applied Fracture Mechanics. 114 (2021) 102981.

[21] H. Kitagawa, S. Takahashi, Applicability of fracture mechanics to very small cracks or the cracks in the early stage, Proc. 2nd ht. Conj. Mech. Behan. Mater. (1976) 627-631.

[22] H. Kitagawa, S. Takahashi, Fracture mechanical approach to very small fatigue crack growth and to the threshold condition, Trans. Japan Sot. Mech. Engrs. 45 (1979) 1289-1303.

[23] H. Kobayashi, Y. Kawada, H. Nakazawa, Initial stage of fatigue cracking in pure titanium under bending and torsion, J. Sot. Mater. Sci. Japan 27 (1978) 859-864.

[24] W. Zhi, C. Hong, X. Zhang, *et al*., Microstructure and thermal shock behavior of ZrB_2-SiC-graphite composite, Mater. Chem. Phys. 113 (2009) 338-341.

[25] X. Zhang, Z. Wang, C. Hong, *et al*., Modification and validation of the thermal shock parameter for ceramic matrix composites under water quenching condition, Mater. Design. 30 (2009) 4552-4556.

[26] A.Z. Wang, X.Y. Zhao, M.X. Huang, *et al*., A quantitative study of flaw/strength response in ultra-high temperature ceramics based on femtosecond laser method, Theor. Appl. Fract. Mech. 110 (2020) 102775.

Figures

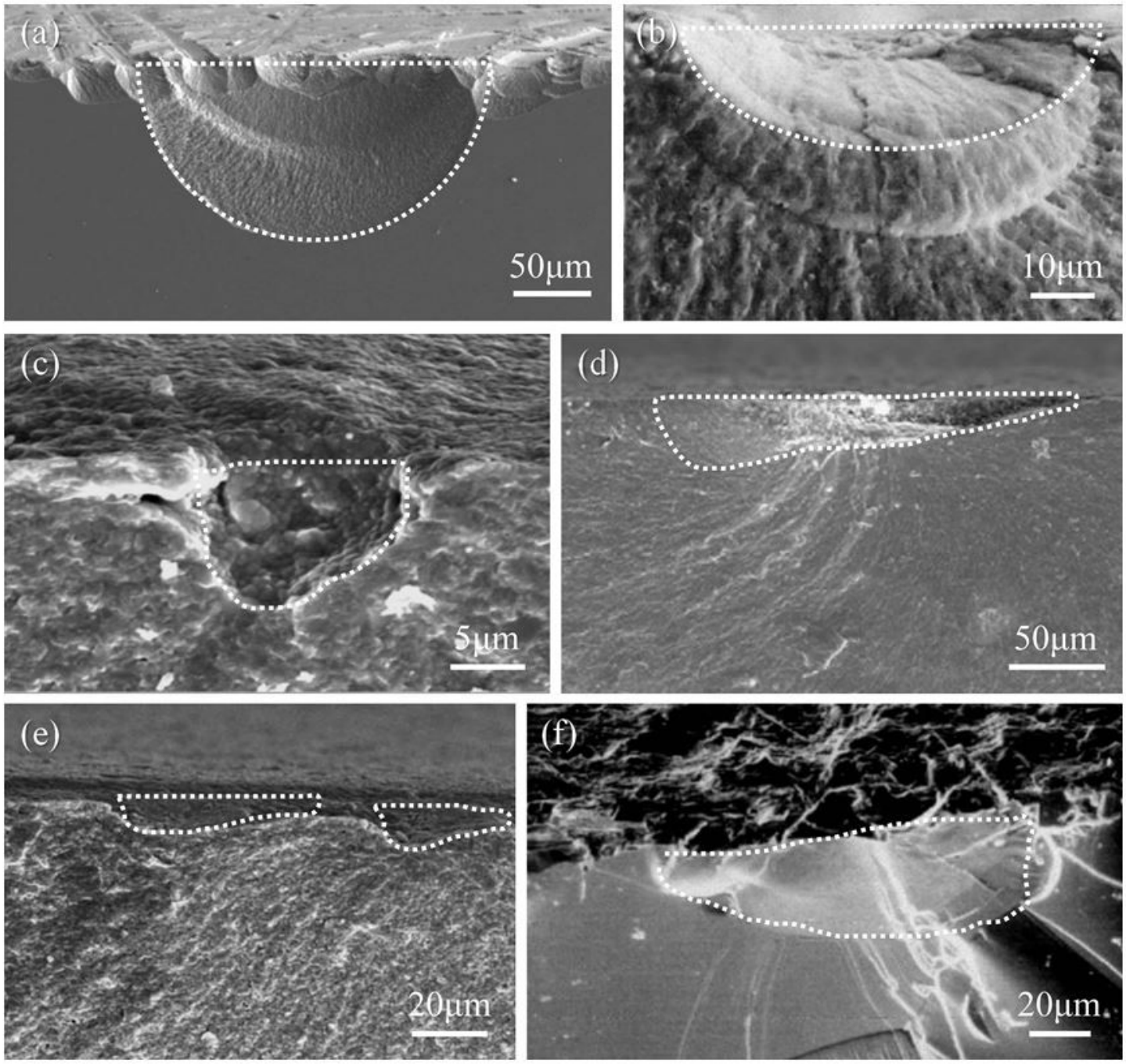

Figure 1

Examples of actual flaws at fracture origins of dense ceramics. (a) edge chipping in 3Y-TZP ceramic [6], (b) critical grinding flaw in fine grain MgAl2O4 [13], (c) surface pore in 3Y-TZP, (d,e) critical grinding flaw in 3Y-TZP [12] and (f) machining chipping in large grain transparent Y2O3 ceramic [13].

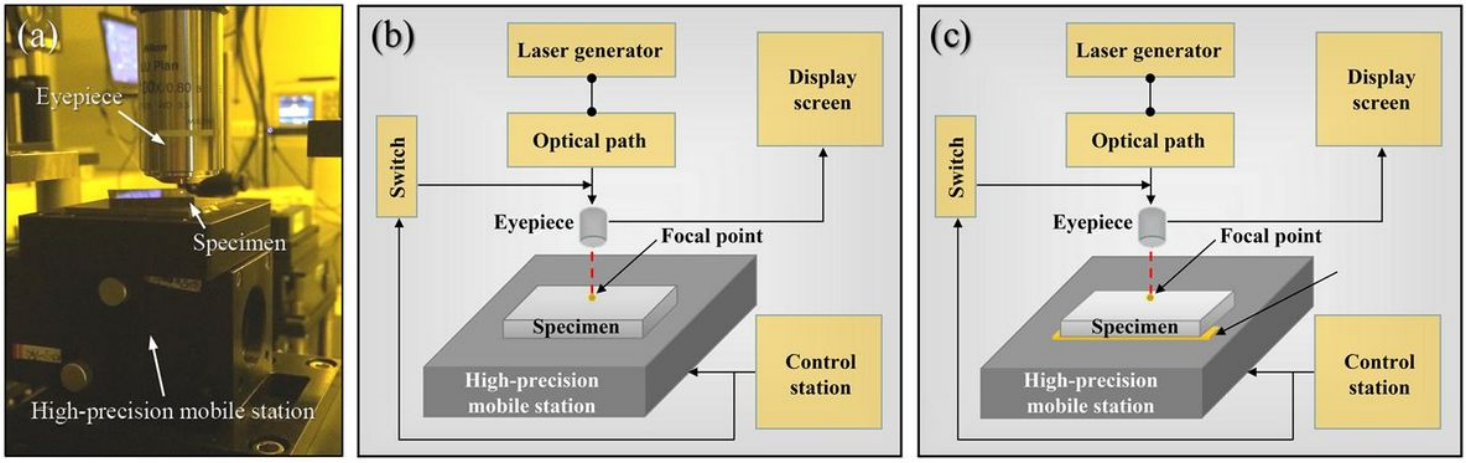

Figure 2

Laser processing method: (a) physical photo and the Schematic diagrams of the introduction of (b) regular as well as (c) irregular flaws.

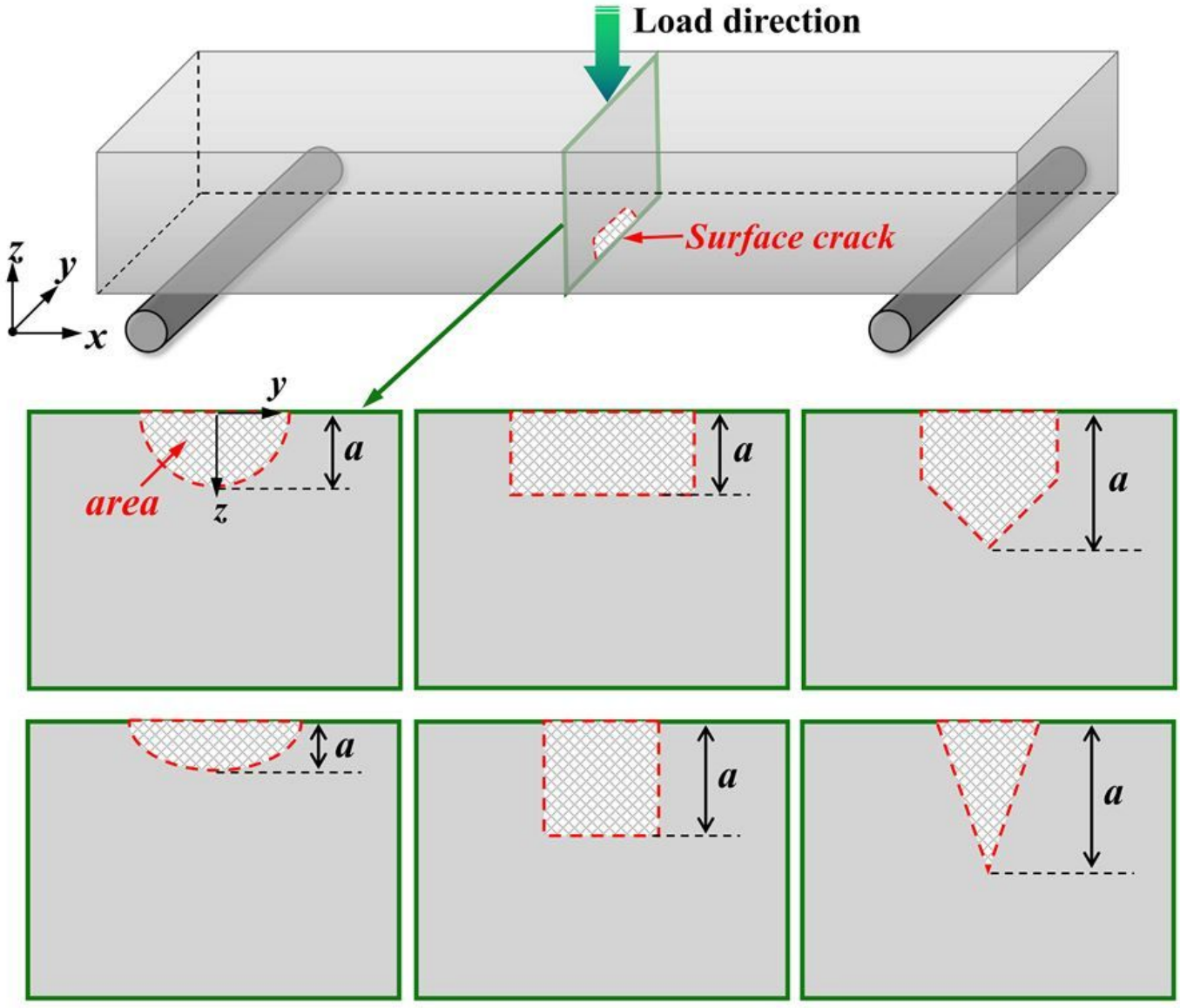

Figure 3

Fracture surfaces of typical cracks with regular and symmetrical shapes.

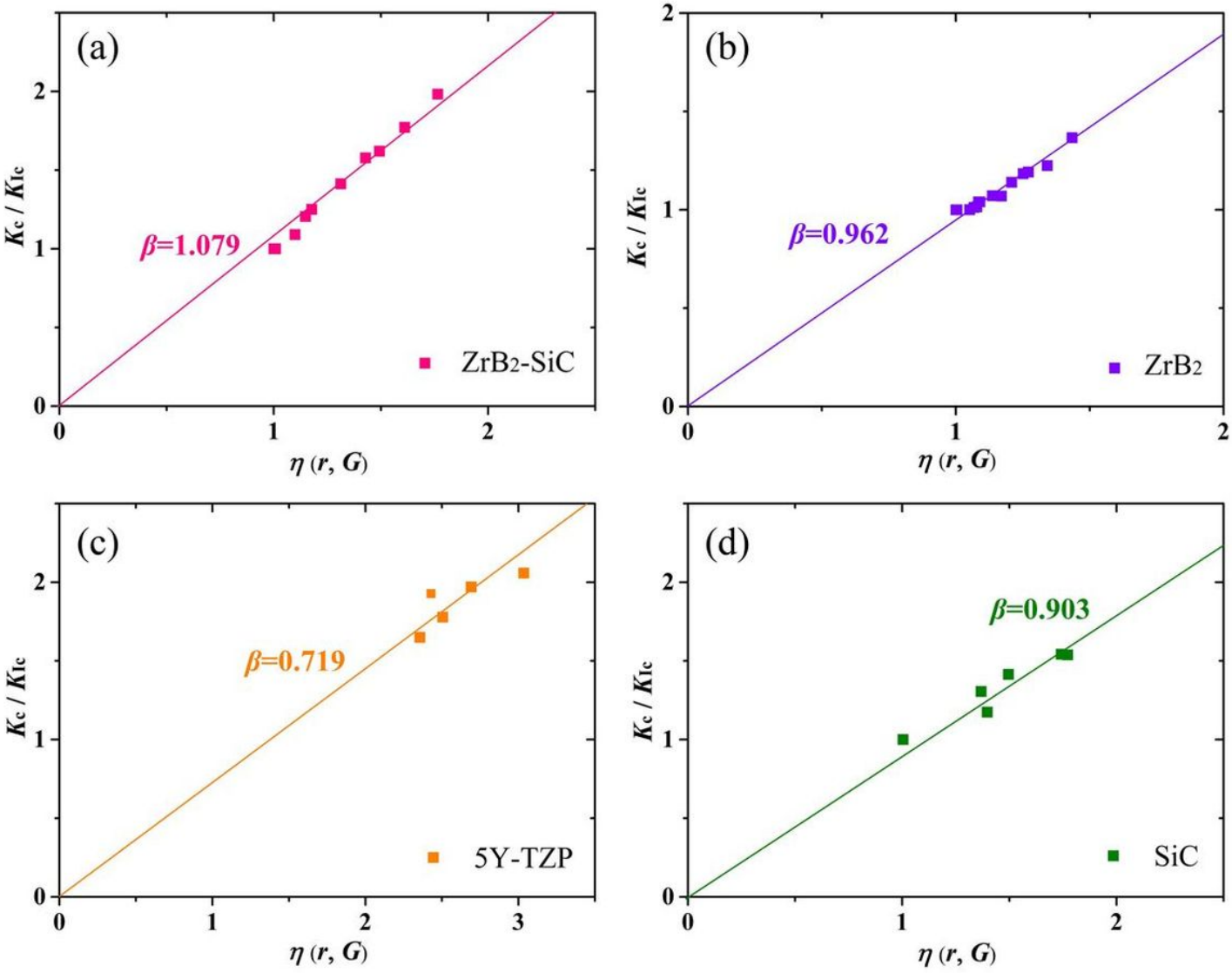

Figure 4

The β values of (a) ZrB2-SiC, (b) ZrB2, (c) 5Y-TZP and (d) SiC ceramics obtained by linear regression.

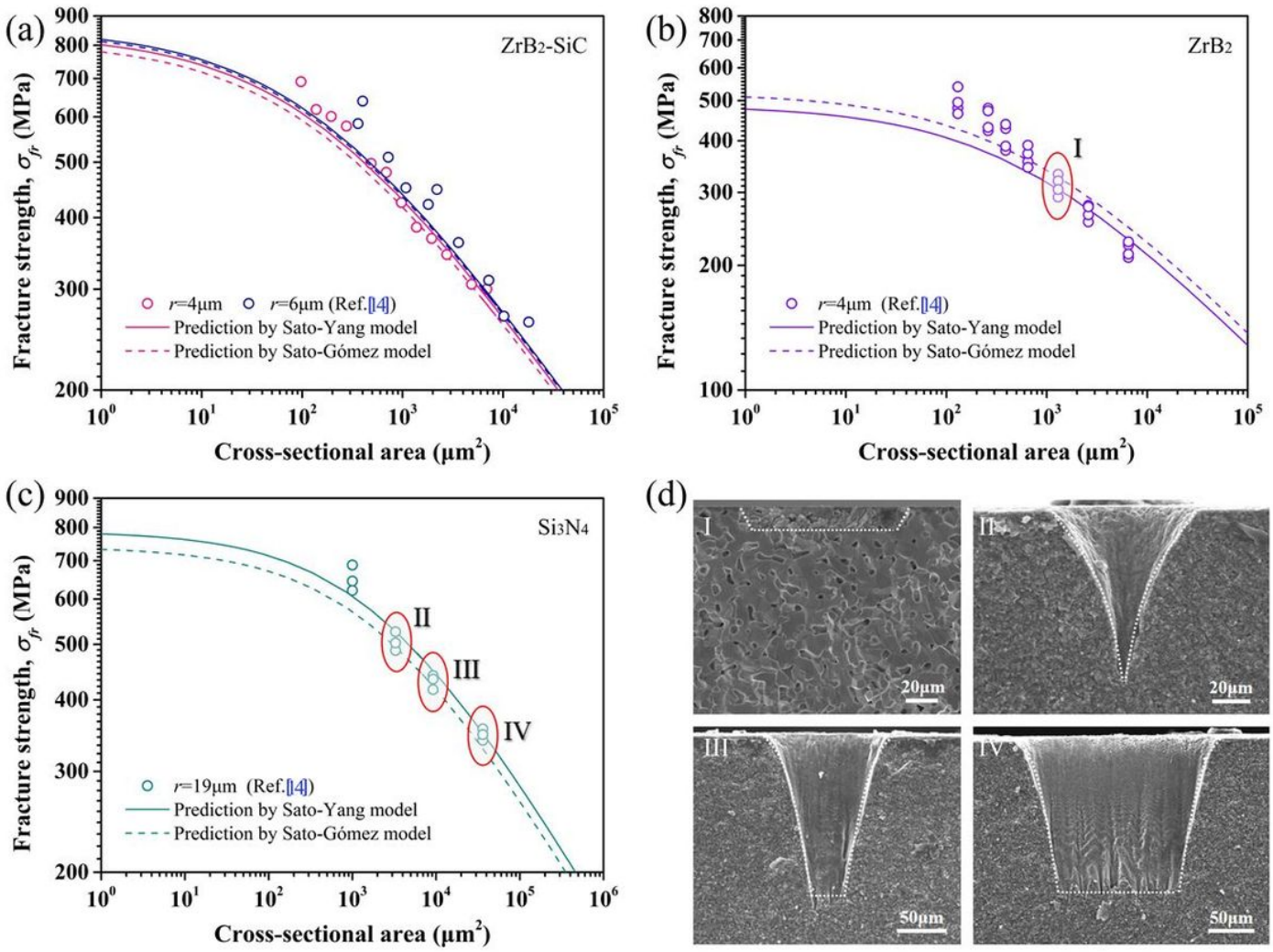

Figure 5

(a-c) Comparisons between the prediction results of the Sato-Yang and Sato-Gómez models as well as the experimental values, and (d) the fracture morphologies of typical test samples.

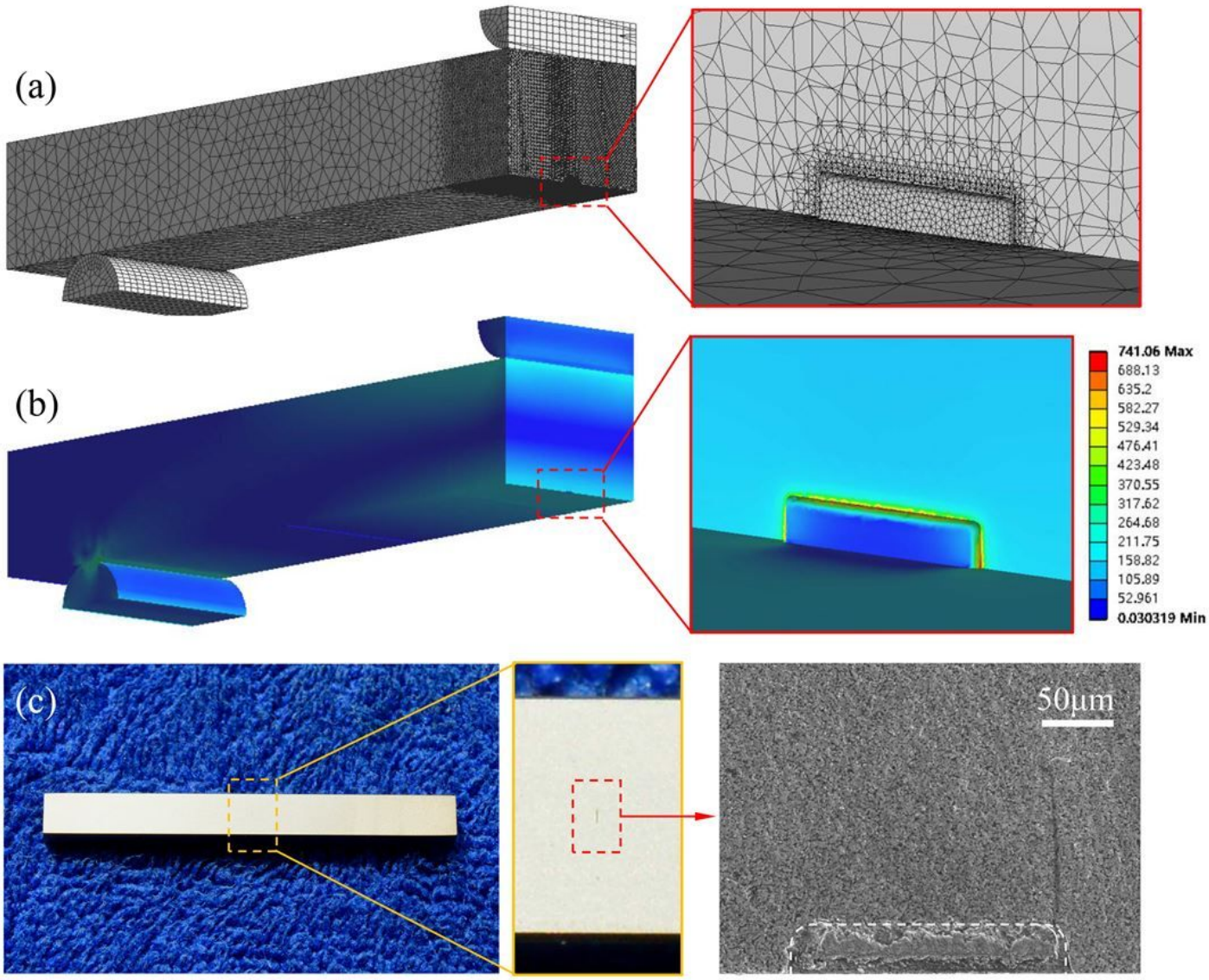

Figure 6

A typical flaw with the length of 200 μm and the depth of 36 μm. (a) Grid distribution in FEM, (b) stress distribution after simulation and (c) the images of the laser-introduced flaw before and after fracture.

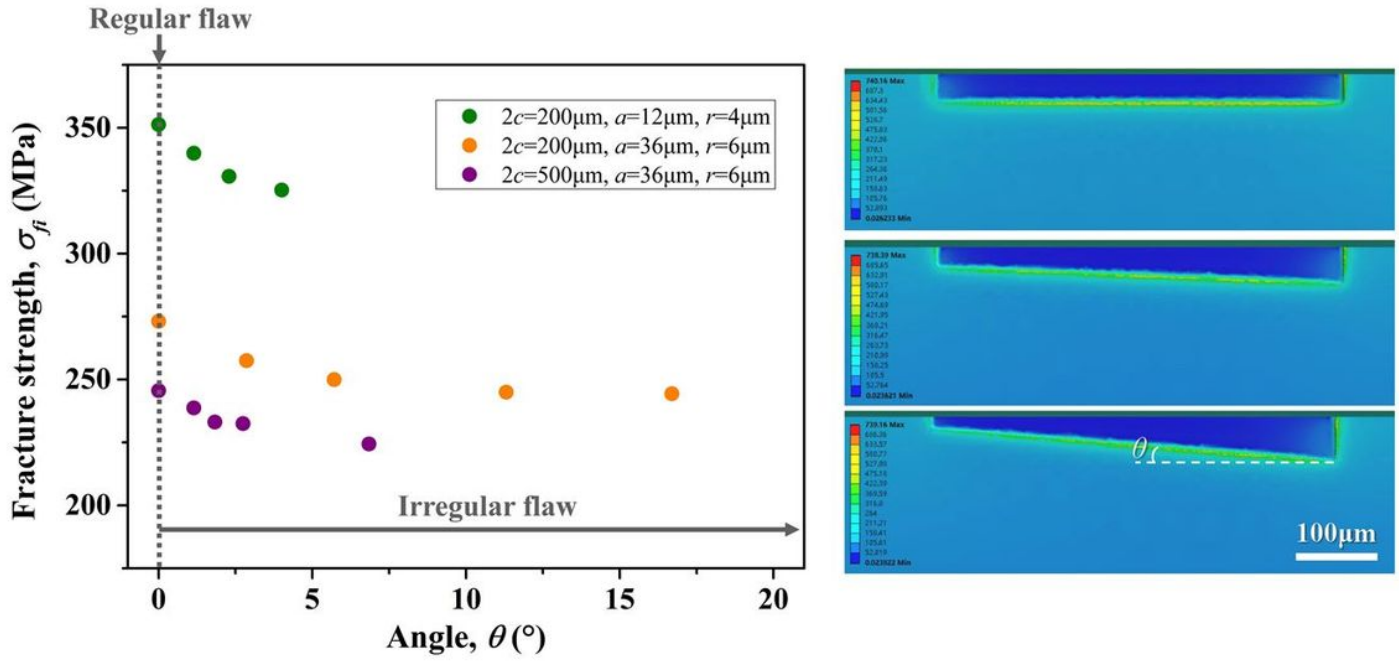

Figure 7

Relationship between the fracture strength caused by irregular flaws (σfi) and the flaw angle θ, and the typical stress distribution cloud diagram.

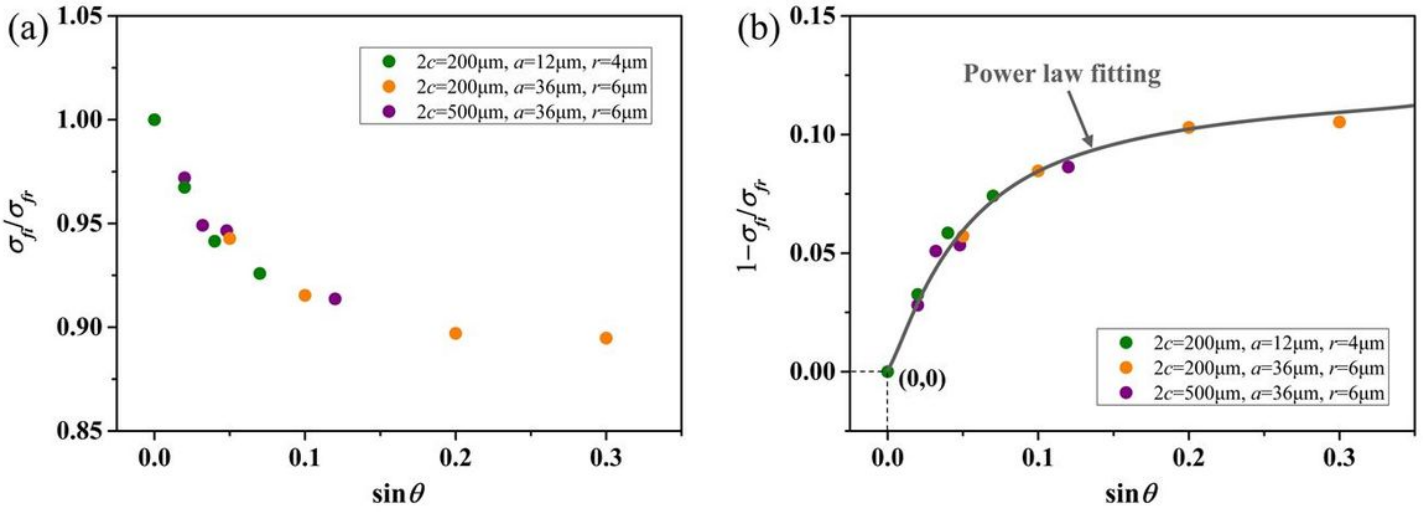

Figure 8

(a) The σfi/σfr vs. sinθ relationship and (b) the power-law relationship between 1-σfi/σf and sinθ.

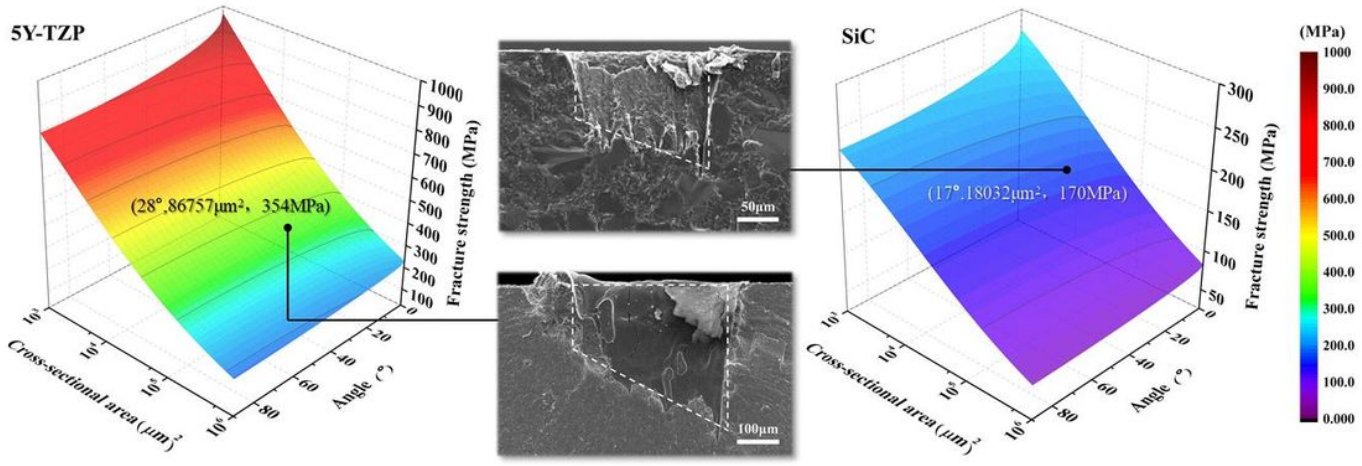

Figure 9

Comparison between the prediction results of the Eq. (4) based on the Sato-Yang model and the experimental values of 5Y-TZP and SiC ceramics.